

# Characterization of personal solar ultraviolet radiation exposure using detrended fluctuation analysis

Suzana M. Blesić<sup>a,b,c</sup>, D. Jean du Preez<sup>d,\*</sup>, Djordje I. Stratimirović<sup>e</sup>, Jelena V. Ajtić<sup>f</sup>,  
M. Cynthia Ramotsehoa<sup>g</sup>, Martin W. Allen<sup>h</sup>, Caradee Y. Wright<sup>d,i</sup>

<sup>a</sup> Institute for Medical Research, University of Belgrade, Belgrade, Serbia

<sup>b</sup> Department of Environmental Sciences, Informatics and Statistics, Ca'Foscari University of Venice, Venice, Italy

<sup>c</sup> Center for Participatory Science, Belgrade, Serbia

<sup>d</sup> Department of Geography, Geoinformatics and Meteorology, University of Pretoria, Pretoria, South Africa

<sup>e</sup> Faculty of Dental Medicine, University of Belgrade, Belgrade, Serbia

<sup>f</sup> Faculty of Veterinary Medicine, University of Belgrade, Serbia

<sup>g</sup> Occupational Hygiene and Health Research Initiative (OHHR), Faculty of Health Sciences, North-West University, Potchefstroom, South Africa

<sup>h</sup> MacDiarmid Institute for Advanced Materials and Nanotechnology, University of Canterbury, New Zealand

<sup>i</sup> Environment and Health Research Unit, South African Medical Research Council, Pretoria, South Africa

## ABSTRACT

### Keywords:

Solar ultraviolet radiation exposure  
Personal dosimetry  
Statistical analysis  
Environmental health

Studies of personal solar ultraviolet radiation (pUVR) exposure are important to identify populations at-risk of excess and insufficient exposure given the negative and positive health impacts, respectively, of time spent in the sun. Electronic UVR dosimeters measure personal solar UVR exposure at high frequency intervals generating large datasets. Sophisticated methods are needed to analyze these data. Previously, wavelet transform (WT) analysis was applied to high-frequency personal recordings collected by electronic UVR dosimeters. Those findings showed scaling behavior in the datasets that changed from uncorrelated to long-range correlated with increasing duration of time spent in the sun. We hypothesized that the WT slope would be influenced by the duration of time that a person spends in continuum outside. In this study, we address this hypothesis by using an experimental study approach. We aimed to corroborate this hypothesis and to characterize the extent and nature of influence time a person spends outside has on the shape of statistical functions that we used to analyze individual UVR exposure patterns. Detrended fluctuation analysis (DFA) was applied to personal sun exposure data. We analyzed sun exposure recordings from skiers (on snow) and hikers in Europe, golfers in New Zealand and outdoor workers in South Africa. Results confirmed validity of the DFA superposition rule for assessment of pUVR data and showed that pUVR scaling is determined by personal patterns of exposure on lower scales. We also showed that this dominance ends at the range of time scales comparable to the maximal duration of continuous exposure to solar UVR during the day; in this way the superposition rule can be used to quantify behavioral patterns, particularly accurate if it is determined on WT curves. These findings confirm a novel way in which large datasets of personal UVR data may be analyzed to inform messaging regarding safe sun exposure for human health.

## 1. Introduction

Some sun exposure, specifically exposure to solar ultraviolet radiation (UVR) has health benefits, such as for vitamin D production (Baggerly et al., 2015). Excess sun exposure, that can lead to sunburn, is associated with melanoma etiology as well as the development of keratinocytic cancers, skin photoaging and certain types of cataract

(Gallagher and Lee, 2006). The global burden of disease attributable to solar UVR exposure is estimated to cause an annual loss of 1.6 million Disability-Adjusted Life Years or 0.1% of the total global disease burden (Lucas et al., 2008). While UVR exposure is considered a minor contributor to the world's disease burden, a large portion of the morbidity and mortality associated with personal solar UVR exposure could be avoided. Sun exposure is a modifiable risk factor in relation to skin

\* Corresponding author.

E-mail addresses: blesic.suzana@gmail.com (S.M. Blesić), dupreez.dj@tuks.co.za (D.J. du Preez), dj.stratimirovic@gmail.com (D.I. Stratimirović), jelena.ajtic@vet.bg.ac.rs (J.V. Ajtić), cynthia.Ramotsehoa@nwu.ac.za (M.C. Ramotsehoa), martin.allen@canterbury.ac.nz (M.W. Allen), Caradee.Wright@mrc.ac.za (C.Y. Wright).

cancer that can be reduced or eliminated by practicing safe sun behaviours and using sun protection in outdoor occupational and recreational settings (Islami et al., 2017).

To develop sun awareness campaigns and to craft messages to assist the public to protect themselves against the adverse effects of excess personal solar UVR exposure, several studies have measured personal exposure to identify at risk groups exposed to high levels of solar UVR (Xiang et al., 2015; Cust et al., 2018; Hacker et al., 2018). Studies have measured personal solar UVR exposure during most types of outdoor activities (O’Riordan et al., 2008; Fernández-Morano et al., 2017) as well as in various occupational settings (Hammond et al., 2009; Wittlich et al., 2016). Several studies have measured personal exposure using personal dosimeters which vary in type and precision, among other factors, and require an appropriate configuration to answer a particular research question (King et al., 2015). In the instance of personal dosimeters, the dosimeters are attached to an individual or to several individuals (depending on the size of the study) and typically measure solar UV-A, UV-B and/or erythematous UV-B radiation. Personal exposures to solar UVR recorded in this way differ from the static ambient UVR data, typically measured on a horizontal surface. Personal UVR data are, in other words, taken on body sites that change in orientation and position with movement, and thus reflect information on individual daily exposure behavior. A major challenge of large personal exposure studies using electronic dosimeters (most commonly used nowadays) is the amount of data acquired and deciding upon the most cost-effective and time-sensitive way to prepare and analyze the data for meaningful interpretation.

In a previous attempt to search for the best methodological and statistical approach to analyze such datasets, we applied wavelet transform (WT) analysis, more precisely wavelet-based spectral analysis (WTS), to high-frequency personal recordings collected by electronic UVR dosimeters designed to measure erythematous UVR exposure (Blesić et al., 2016). The analysis of our WTS results showed that personal datasets can be characterized by a long-range temporal behavior, that changed from uncorrelated to long-range correlated with increasing duration of time spent in the sun. WT spectral peaks also suggested the existence of characteristic times in sun exposure behavior that seemed to be universal across the dataset at the time. It was also possible to use WT to classify groups of records in terms of distinct individual UVR exposure patterns previously not done using conventional statistics (Blesić et al., 2016). One aspect of the previous study that warranted further research came about from the analysis of data from construction site workers in New Zealand. It showed that WT slopes could still be different for individuals who spent almost the same amount of time outside and had very similar daily sun exposure, and thus the same or very similar classical statistical measures of exposure behavior. We hypothesized that the WT slope would be influenced by the duration of time that a person spends in continuum outside. In this study, we addressed this hypothesis by using an experimental study approach. We aimed to corroborate this hypothesis, and to assess and characterize the extent and the nature of influence the time a person spends outside has on the form of statistical functions that we used to analyze individual UVR exposure patterns. To this end, we applied the detrended fluctuation analysis (DFA), previously only used for ambient solar UVR measurements (Da Silva Filho et al., 2016), to personal sun exposure data.

## 2. Data and methods

### 2.1. Data and data collection

Data from several different activities located in different geographic sites (see Table 1) were used in this study to provide a wide variety of exposure patterns. At each location, participants wore the electronic dosimeter badges while they engaged in their various activities and at least one dosimeter badge was used to measure ambient UVR at each

**Table 1** Summary of experiments of conducted using the dosimeter badges.

Location	GPS (°)	Altitude (m)	Activity	Date (mean seasonal temperature, in °C)	Number of participants (age range in yrs)	Dosimeter positions	Recording frequency	Number of data points per day (N)
Pretoria, South Africa	-25.77, 28.21	1433	Inside/outside simulation	November 16, 2016 (19.1)	-	-	1 min	720
Potchefstroom, South Africa	-26.68, 27.08	1368	Car guard	September 18, 2017–September 22, 2017 (14.6)	8 (33–55)	Wrist	1 min	840
Val Cenis, France	45.21, 6.53	2143	Skiing	January 29, 2017–February 3, 2017 (0.4)	11 (12–50)	Hard hat, glasses, arm	1 min	1440
Stara Planina, Serbia	43.24, 22.33	921	Skiing	December 31, 2016–December 8, 2017 (0.5)	7 (12–50)	Hard hat, glasses, arm	1 min	1440
Dolomites Mountains, Italy	46.43, 11.55	1999	Hiking	July 23, 2018–July 26, 2018 (21.3)	3 (6–47)	Wrist	8 s	1800
Avondale, New Zealand	-36.89, 174.69	12	Golf	March 01, 2017 (15.6)	1 (-)	Chest, wrist, head	2 s (golfing) and 4 s (ambient)	7200 (golfing) and 3600 (ambient)

location. The badge used to measure ambient UVR was placed on a horizontal surface so that it would receive total exposure for the entire day. For each experiment, the dosimeter badges used a sampling rate of 60 s except for the hiking experiment, which used an 8-s sampling interval, and a golfing experiment that used 2- and 4-s sampling. The dosimeter badges used were designed to measure erythemal exposure in the wavelength range of 290–400 nm. A solid-state detector with a linear response to UVR was used to measure erythemal UVR. The angular response of the instrument is close to that of the cosine response of human skin due to the weatherproof case over the detector. The same dosimeter badges have successfully been used in previous exposure studies; more details on specifications and functioning of the dosimeter badges are provided elsewhere (Allen and McKenzie, 2005; Wright et al., 2007; Seckmeyer et al., 2012). All the badges gave records in dimensionless counts that could be converted to Ultraviolet Index (UVI) units after a calibration against the meteorological-grade instrument that measures UVR (please see explanation in Blesić et al. (2016) and references therein).

Of all the recordings, the inside-outside experiment (IO) was not related to any specific individual behavior but was designed to simulate personal exposure to solar ultraviolet radiation (pUVR) for 15-min, 30-min, 1-h, and 2-h IO signals. In other words, for the IO experiment we placed dosimeter badges successively inside and outside at 15-min, 30-min, 1-h, and 2-h intervals on the same day. We devised this experiment to see how this highly regular, periodic pattern of ‘behavior’ would reflect in the statistical functions we applied.

For some of the experiments, the counts for the dosimeter badges were converted to erythemally-weighted UVI using the following equation:

$$UVI = k_{er} \times \int_{250 \text{ nm}}^{400 \text{ nm}} E_{\lambda} \times S_{er}(\lambda) d\lambda,$$

where  $E_{\lambda}$  is the solar spectral irradiance at wavelength  $\lambda$  in  $\text{W}/\text{m}^2/\text{nm}$ ,  $k_{er}$  is equal to  $40 \text{ W}/\text{m}^2$  and  $S_{er}$  is the CIE reference erythemal action spectrum. The UVI data points were then integrated over the time period and converted to standard erythemal dose (SED) units to determine the total UVR received during the day (Blesić et al., 2016).

### 3. Methods

We characterized time series of personal exposure to solar UVR (pUVR) by calculating the scaling (or long-range, or long-memory, or Hurst) exponent  $\alpha$  of the 2nd order detrended fluctuation function (DFA2) that is a result of the detrended fluctuation analysis (DFA) with linear trends in the data systematically removed. DFA was introduced as an appropriate statistical approach to deal with any nonstationary record that contains some trends of unknown form (Peng et al., 1994). In DFA, the procedure of detrending was devised to eliminate such trends; the resulting remarkable performance of this method, proven by numerous systematic studies (Hu et al., 2001; Chen et al., 2002, 2005; Xu et al., 2005; Bashan et al., 2008) and across different fields (Stanley, 2000) stems from its highly effective detrending solution.

The DFA procedure (Peng et al., 1994) for the analysis of any discrete, recorded time sequence  $A(k)$  ( $k = 1 \dots N$ ), where  $N$  represents the total number of data recorded, requires three consecutive steps. In the first step, for each time series  $A(k)$ , the partial sum  $y(n) = \sum_{k=1}^n A(k) - \bar{A}$  is calculated, with  $\bar{A}$  being the average value of the recorded variable for the entire record. Next, the entire series of  $y(n)$  is divided into a set of overlapping segments (Buldyrev et al., 1995) of the length  $l$  and the local trend for each segment, the linear or polynomial least-squares fit for the segment data, is calculated. The order  $m$  of polynomial that defines the local trend represents the order of DFA method (DFAm) - here we used DFA2. A sliding segment of size  $l$  produces new series of segments with the detrended sequences  $y_{l,i}(n)$  ( $1 \leq i \leq (N-l+1)$ ) that are differences between original series  $y(n)$

and the local trend. Finally, DFA2 fluctuation function is obtained as the average of variances about the local trend for each segment, over all segments, as  $F(l) = \sqrt{\frac{1}{(N-l+1)l} \sum_{i=1}^{N-l+1} \sum_{n=1}^l y_{l,i}(n)^2}$ .

This procedure design renders DFA an optimal statistical approach to use in analysis of natural or human-made nonstationary data compared to calculations of autocorrelation function (ACF) or Fourier power spectra (PwS). Namely, a) by way of subtracting local trends at different time window lengths  $l$ , DFA produces a time series that fluctuates much less than the original, and still has the same statistical properties (Stanley, 2005) and b) DFA is, by definition, a sum over autocorrelations (Höll and Kantz, 2015) thus fluctuates less than the typical autocorrelation function and is markedly more stable in data analysis (Bunde et al., 2013).

If the analyzed records are statistically long-range autocorrelated, or long-term persistent (LTP), due to their inherent power-law data dynamics, DFA2 function behaves as  $F(n) \sim n^{\alpha}$ , with  $0.5 < \alpha \leq 1$ ; if the time series  $A(k)$  is short-range autocorrelated, or has no correlations at all,  $\alpha = 0.5$  (Peng et al., 1994). In this way, DFA2 presents as a straight line on log-log graphs of dependence of  $F(n)$  of the time scale  $n$ , allowing for quantification of the so-called scaling, or long-range autocorrelated character of data by the corresponding power-law exponent  $\alpha$ . Instances when  $\alpha > 1$  imply the existence of intrinsic non-stationarities in autocorrelated data (Höll et al., 2016). Finally, for LTP records the corresponding Fourier PwS decreases as a power law as well, in the form  $E_F(\omega) \sim \omega^{-\beta}$ , and the exponent  $\beta$  that can be directly related to the DFA exponent  $\alpha$  through the scaling relation  $\beta = 2\alpha - 1$  (Peng et al., 1993).

It has been shown by other groups (see, for example, the early investigations by Mandelbrot and Wallis (1969)) and by us (Blesić et al., 2018) that a pure LTP behavior rarely occurs in natural records, and thus the corresponding DFA2 functions, depicted on the log-log graphs, are rarely ideal linear functions. Instead, they usually contain transient crossovers in scaling that arise from presence of irregularities of different types (Mallat and Hwang, 1992; Hu et al., 2001) most commonly the effects of mixtures of cyclic components that locally perturb DFA2 functions (Mandelbrot and Wallis, 1969). When these transient crossovers appear in DFA2 functions they cannot, however, be used to accurately determine characteristic times, or the periods, of the cyclic phenomena that have caused them. Numerical studies with artificially-generated time series with added trends (Hu et al., 2001) demonstrated that, due to the DFA design, positions and spread of any such perturbation on DFA2 varies depending on the scaling exponent  $\alpha$  and the period and/or amplitude of the hypothetical periodic trend (Mandelbrot and Wallis, 1969; Hu et al., 2001). For this reason, when the effects of such irregularities are visible in DFA2 functions, we used wavelet transform power spectral (WTS) analysis to investigate them in detail.

The wavelet transform (WT) analysis was introduced (Morlet et al., 1982; Grossmann and Morlet, 1984) to circumvent the uncertainty principle problem in classical Fourier transform analysis (Stratimirović et al., 2018) and achieve better signal localization in both time and frequency. In WT, the size of an examination window is adjusted to the frequency analyzed; in this way an adequate time resolution for high frequencies and a good frequency resolution for low frequencies is achieved in a single transform (Bračič and Stefanovska, 1998). For a detailed explanation of the WTS procedure that we used in this paper we refer to the original articles that introduced WT and WTS, e.g. Morlet et al. (1982) and Astafeva, (1996), or studies that have applied WTS, e.g. Stratimirović et al. (2001). Here, we calculated the wavelet power spectra  $E_W(n)$  which can be related to the corresponding Fourier power spectra  $E_F(\omega)$  via the formula (Perrier et al., 1995) that stipulates that if any of the two spectra -  $E_W(n)$  or  $E_F(\omega)$  - exhibit power-law behavior, then the other will be of the power-law type too, with the same power-law exponent  $\beta$  (Stratimirović et al., 2001). This means that WTS can have a dual function in time series analysis - it calculates

contribution to signal energy along the scale of  $n$  in the same way as the classical Fourier spectrum, thus providing information on cyclic influences within data, and provides the information on scaling, through the value of  $\beta$ , confirming or challenging DFA2 scaling results (that is, the obtained values of  $\alpha$ ). We used Morlet wavelets of the 6th order and Paul wavelets of the 4th order as wavelet bases for our analysis for they are well adapted to accurately estimate characteristic times or periods of local irregularities of analyzed time series (Mallat and Hwang, 1992). They are, by definition, narrow in spectral (scale)-space, and broad in the time-space, which results in very well localized, relatively sharp peaks in the global WT spectra (Torrence and Compo, 1998) that may mark appearances of periodic or non-periodic cycles, or even significant singular events in the analyzed time series (Mallat and Hwang, 1992).

We calculated DFA2 and WTS functions for our pUVR data and plotted them on a double logarithmic scale to estimate values of  $\alpha$  and  $\beta$  by linear fits. Due to the finite sample size effects, and following recommendations by Hu et al. (2001), Kantelhardt et al. (2001), Bashan et al. (2008), Ludescher et al. (2017) and Koscielny-Bunde et al. (2006), we considered only values of DFA2 and WTS between the minimum time scale of  $n = 5$  for DFA2 and  $n = 2$  for WTS and the statistically meaningful maximum time scale of  $n = N/10$ ; this defined the range of scales available for our analyses. We recalculated scale  $n$  into time  $t$  for presentations in graphs below; this was not done only if measurements of different recording frequencies were presented together, in order to avoid horizontal shift in time scale.

#### 4. Results

We aimed to test and explain our hypothesis that, even if the amount of total exposure to solar UVR is a factor influencing the values of  $\alpha$  and  $\beta$  of DFA2 and WTS slopes, it is the duration of repeated or single patterns of continuous exposure that will result in larger  $\alpha$  and  $\beta$  - that is, in more pronounced LTP of pUVR data. First, we analyzed simulated pUVR data from the IO experiment. For all the records in our IO sample we calculated DFA2 and WTS functions. Assuming that any recorded pUVR signal is a superposition, or result of a combination of the ambient solar UVR and a personal pattern of outside behavior, we also calculated differences  $F_p = \sqrt{F_{pUVR}^2 - F_{out}^2}$  and  $E_{W,p} = E_{W,pUVR} - E_{W,out}$ , where  $F_{pUVR}$  and  $E_{W,pUVR}$  represent DFA2 functions and WTS spectra of our recorded pUVR data, while  $F_{out}$  and  $E_{W,out}$  stand for DFA2 and WTS results for the corresponding ambient UV records. We did this following systematic assessments of effects of trends and non-stationarities on DFA of artificially-generated time series given in Hu et al. (2001) and Chen et al. (2002). These papers provide a theoretical superposition rule devised to describe DFA functions of data artificially constructed by mixing signals with different scaling exponents  $\alpha$ ; superposition rule states that, for a time series comprised of segments of mutually-independent (non-correlated) signals  $f(t)$  and  $g(t)$ , the DFA function (of any order) can be calculated as  $F_{f+g}^2 = F_f^2 + F_g^2$ , where  $F_f$  and  $F_g$  are the DFA functions of signals composed of only the segments  $f(t)$  or  $g(t)$  and segments of different correlations substituted with zeros. Following relations that connect DFA function and Fourier (and thus also WT) power spectra (Kiyono, 2015), the same superposition rule leads to relation  $E_{W,f+g} = E_{W,f} + E_{W,g}$ . In the case of our datasets, following the premise of the superposition rule,  $F_p$  and  $E_{W,p}$  represent DFA2 and WTS functions of a ‘personal’ signal, defined solely by the pattern of individual outside behavior.

In Fig. 1 we present recorded UVR data from our IO experiment (Fig. 1A), together with the results of their DFA2 analysis (Fig. 1B). The DFA2 functions of the 15-min, 30-min, 1-h, and 2-h IO signals all present visible change in scaling behavior that transfers to larger scales with the increase of time spent inside/outside (for clarity of display, we have only presented the 15-min and 30-min results in Fig. 1B). In addition, the application of the superposition rule to IO DFA2 functions

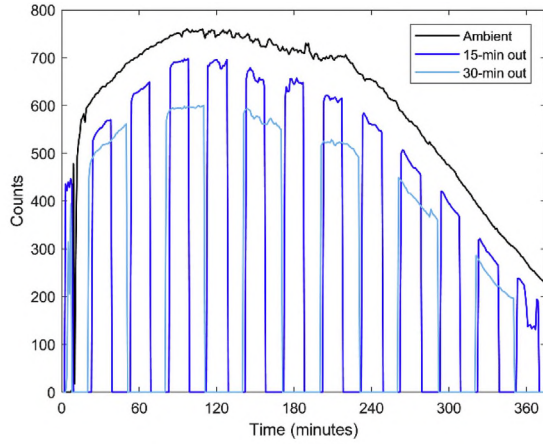
shows that the lower part of DFA2 functions is dominated by the simulated pattern of outside behavior, while the upper part, in the range of time scales after the transient crossovers in scaling, is dominated by ambient UVR. The duration, or the range of scales, of pattern dominance of outside behavior (or ‘personal’ behavior) on the pUVR DFA2 is, as expected, longer for longer continuous exposure to solar UVR, even if the total exposure of all the analyzed records is the same. This also seems to affect the values of  $\alpha$  for different DFA2 functions in the same manner – longer exposure leads to larger values of  $\alpha$ . We cannot, however, calculate exponents  $\alpha$  precisely for our IO data due to the profound dominance of periodic trends (caused by 15-min, 30-min, 1-h and 2-h IO patterns). Hence, the accurate estimation of scaling is impossible unless these influences are firstly removed from records (Blesić et al., 2018).

In Fig. 2 we present WTS results that we obtained for all the IO data. The WTS functions present with the prominent cycles at 30-min, 60-min, 120-min and 240-min intervals, corresponding to the full periods of a 15-min, 30-min, 1-h and 2-h patterns. The application of the superposition rule illustrates the dominance of personal patterns of outside behavior in the lower scales, up until the end of cyclic peak intervals. Finally, even if, as in DFA2, accurate estimation of scaling exponents  $\beta$  is hindered by the prominent effects of cycles, it is visible that the slopes of WTS functions do rise with the duration of continuous exposure to the solar UVR as predicted. Thus, results of the IO experiment, presented in Figs. 1 and 2, confirm that a) LTP of the pUVR records is more prominent with longer repeated continuous exposure to solar UVR, and b) durations of repeated continuous exposures in the record can correctly be extracted from the ‘personal’ DFA2 and WTS functions calculated by using the superposition rule.

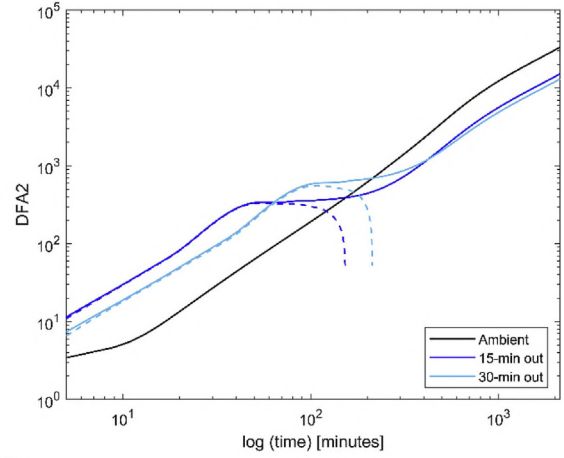
We further tested the validity of these findings for cases of pUVR records obtained from the car guards, skiers, hikers and golfers measurements.

Fig. 3 shows illustrative examples of the original data (panel A), together with their DFA2 (panel B) and WTS (panel C) results, for the car guards measurements. In Fig. 3B we give DFA2 functions for the original pUVR records, superposition ‘personal’ DFA2 (calculated as  $DFA2_p = \sqrt{DFA2_{pUVR}^2 - DFA2_{out}^2}$ ), and superposition ambient DFA2 (given as  $-DFA2_p$ ). The corresponding WT results are presented in Fig. 3C. Fig. 3A also provides information on the total daily exposure (given in SED units) and total daily exposure time (total time spent outside,  $tt$ ) for the illustrated measurements. As in the IO case, car guards results with higher LTP are accompanied with a corresponding  $DFA2_p$  that covers the initial part of the curve and reaches longer time scales. This means that, if the superposition rule stands in the pUVR case, a longer continuous exposure to solar UVR is connected to the larger LTP, unrelated to the amount of total exposure. The WTS graphs (Fig. 3C) can help determine the amount of time of the longest duration of total exposure the person had that day by searching for the last visible cycle covered by the  $E_{W,p}$  curve. Due to ability of WTS to register both periodic and non-periodic cycles and durations of significant singular events, cycles in  $E_{W,p}$  functions can inform the duration of the repeated exposure pattern(s), as in IO experiment, or the duration of a singular continuous significant exposure. The form of  $E_{W,p}$  can thus partially explain individual patterns of outside behavior. Fig. 3C also suggests that perhaps these cycles in WTS functions, defined by durations of continuous time spent outside, dominantly drive DFA2 and WTS behaviors on lower time scales. Finally, Fig. 3 additionally provides values of scaling exponents  $\alpha$  and  $\beta$ . We provide values of  $\beta$  in a form  $\alpha_\beta = (1 + \beta)/2$ , to enable comparison of the two scaling exponents according to their scaling relation (Peng et al., 1993). It is important to note that for the cases presented in Fig. 3, and for the rest of the dataset, values of  $\alpha$  and  $\beta$  (that is,  $\alpha_\beta$ ) align within the range of error which depends on the number of data points  $N$  and here is equal to 0.04 (Bashan et al., 2008).

The skiing dataset results, presented in Fig. 4, confirm this finding.



A



B

**Fig. 1.** (A) Recorded UVR series from the IO experiment for the 15-min and 30-min consecutive inside-outside repositioning of UV dosimeters, together with the ambient recording for the same time period. (B) DFA2 results of the inside/outside experiment with the dashed lines representing the superposition of the respective result.

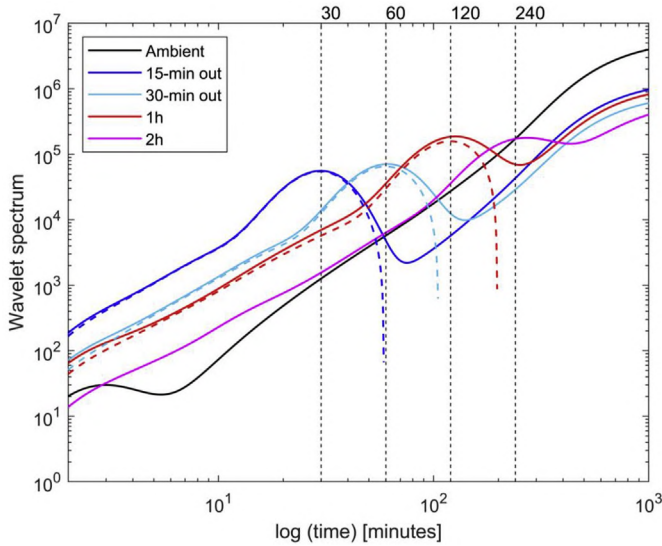


**Fig. 2.** Wavelet transformation results of the inside-outside experiment calculated with the use of Paul wavelets. Dashed lines represent superposition of the respective result. Vertical lines at 30, 60, 120, and 240 min are given as visual guides.

Two cases are shown in Fig. 4, one of a person who spent a long time outside continuously, and another of a person who was outside randomly in short time intervals. The DFA2 results confirm previous observations of the connection between values of  $\alpha$  and duration of continuous exposure. The WTS results confirm that the cycles that define durations of exposure define slopes  $\alpha$  and  $\beta$  on lower scales. In the case of both skiers, the appearance of multiple such cycles exists that in the case of the ‘very active’ skier even define the whole DFA2-WTS behavior in the range of scales available in our analyses. For this person, we are probably observing a combination of personal exposure patterns, in which the ‘personal’ cycles on lower time scales (at around 10 min, 20 min, and 30 min) possibly mark repeated continuous exposure, while the peaks at very long scales (in the range of 60–90 min) could be derived from a single continuous significant exposure.

In Fig. 5 a combination of hikers and golfer recordings were used to illustrate how the DFA-WTS superposition rule may be used to analyze specific groups of outside behaviors (in this case, recreational activities). In panels A and B of Fig. 5 the original records of hiking and

golfing pUVR are shown, together with the ambient data for the recording period. The recording periods cover only the period of a specific activity and are chosen to be of the same duration. During the entire recording time, participants who wore UVR dosimeters were constantly outside. Panels C and D present DFA2 results for the pUVR and the ambient records in two cases, which show how the slopes  $\alpha$  of pUVR data are always lower than those for the corresponding ambient records. Panels E and F depict results of DFA2-WTS comparisons of two sets of pUVR records, with functions derived from the superposition rule to understand personal patterns of behavior. Panel E confirms that longer continuous exposure results in larger slopes of DFA2-WTS functions: from the original records (given in A and B) it was apparent that the golfer spent longer continuous periods exposed to solar UVR which translates to larger value of  $\alpha$  for this pUVR measurement. This is confirmed in panel F, where a prominent cycle of about 20–25 min dominates golfer’s personal WTS, compared to 6–7 min cycle in hiker’s data. Both cycles probably suggest a repeated personal pattern of outside exposure. Due to the very high frequency of hiking and especially golfing recordings (see Table 1) and the finite size effects, we were not able to calculate DFA-WTS functions for longer time intervals and thus examine possible appearance of WTS peaks on larger time scales in the golfer’s data that would suggest long continuous significant singular exposure.

Finally, we investigated whether the improvement in frequency of recording introduces changes to DFA-WTS results. We used golfer’s data for this exercise since these were measured with the highest frequency. From these 2-s-interval data we produced 1-min averages of the original golfing series. The results of comparison of WTS analyses for these two sets of time series are given in Fig. 6. The change in recording frequency does not change shapes of WTS functions for ambient or pUVR data, but only improves (with improved frequency) the details in shape of the WTS function derived from the superposition rule.

## 5. Discussion

Detrended fluctuation analysis (DFA), in combination with the wavelet transform spectral analysis (WTS), was used to assess long-term properties of various pUVR time series. We aimed to quantify their overall LTP and to use the DFA superposition rule (Hu et al., 2001; Chen et al., 2002) to discriminate between different behavioral patterns within the group of records with similar total daily exposures to solar UVR. The DFA superposition rule (Hu et al., 2001; Chen et al., 2002) that was originally devised to describe effects of trends, including

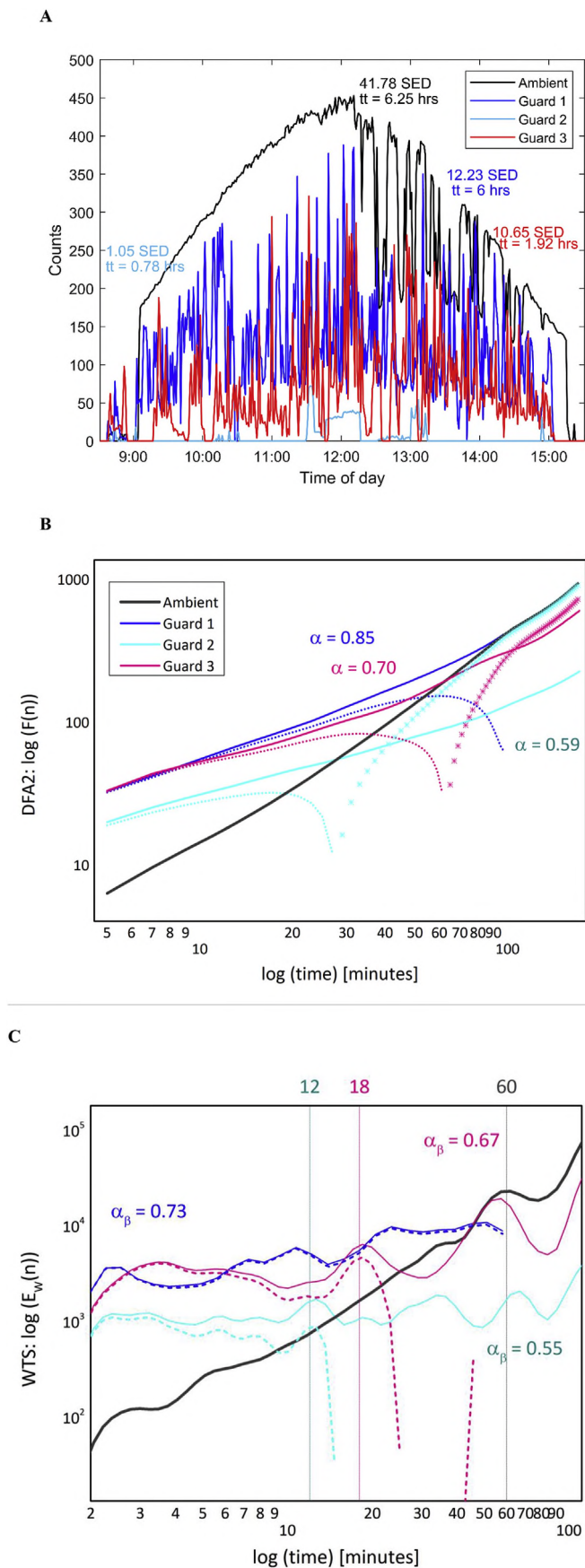


**Fig. 3.** (A) Illustrative examples of the recorded pUVR series from the South African car guards measurements, together with the ambient recording for the same day. Values of the total daily exposure (in SED) and total exposure time ( $tt$ ) for the three cases presented are given. (B) DFA2 results of the CG pUVR data given in (A) (solid lines), with the ‘personal’ contributions to DFA2 functions extracted using the superposition rule (dotted lines) and estimated ‘ambient’ or ‘outside’ influences (asterisks). Values of scaling exponents  $\alpha$  for the three pUVR time series are given. (C) WTS results for the same sets of records, calculated with use of Morlet wavelets. Vertical dotted lines represent WTS estimates of the longest duration of continuous exposure for the analyzed pUVR data. Values of WTS exponents  $\beta$  are given in a form  $\alpha_\beta = (1 + \beta)/2$  so that those can be directly compared with values of scaling exponents  $\alpha$  given in (B).

periodic or aperiodic cyclical influences, on artificially generated time series, has so far been proven valid for use in some instances of analysis of complex signals, including meteorological data (Jun et al., 2006; Blesić et al., 2018).

To test usability of the DFA superposition rule for pUVR records, IO data were analyzed. Our results confirmed validity of the superposition rule to assess pUVR data and showed that the pUVR scaling on lower time scales is determined by personal patterns of exposure. We also showed that this dominance ends at the range of time scales comparable to the maximal duration of repeated or singular continuous exposure to solar UVR during the day. In this way, the superposition rule can be used to quantify behavioral patterns, particularly accurate if it is determined on WTS curves. This is, to our knowledge, is the first result of this kind.

In addition to confirming our previous findings (Blesić et al., 2016) that longer overall daily exposures are reflected in higher DFA2 or WTS slopes, our analysis of the car guarding, skiing, hiking and golfing data also confirmed the IO finding. There exists a difference between slopes (that is, values of scaling exponents  $\alpha$  or  $\beta$ ) for the same (or very similar) total daily exposures, but different durations of maximal continuous exposures during the analyzed day. In our experiments, the maximal duration of exposure additionally raised values of  $\alpha$  or  $\beta$  informing on different patterns of repeated individual behavior. This designates DFA and WTS as additional methods to the classical pUVR analysis methods such as heuristic search algorithms, statistical data processing and supervised/unsupervised machine learning. DFA and WTS can be used as tools to describe and quantify personal exposure behavior and delineate individual outside activity from meteorological data. These methods will prove useful in environmental and behavioral epidemiological studies and to understand more precisely the relationships between pUVR and sun-related health outcomes. This is especially important among vulnerable groups such as children, the elderly and people with pre-existing conditions such as immunosuppression, photophobia and albinism.

## 6. Conclusions

In summary, DFA and WTS are valuable tools to apply in the investigation of pUVR measurements. Outcomes of these types of analyses for ‘big data’ from around the world may be invaluable to understand the present and future health risks associated with sun exposure. Future studies may consider pooling data from multi-site, multi-country studies and using the methods described here to generate results to fine-tune safe sun exposure public health campaigns as well as personal sun prediction modelling tools.

## Acknowledgments

CYW receives research funding from the South African Medical Research Council and the National Research Foundation of South Africa. SB received funding from the European Union’s Horizon 2020 Research and Innovation Programme under the Marie Skłodowska-Curie Grant Agreement 701785. Wavelet software was provided by C.

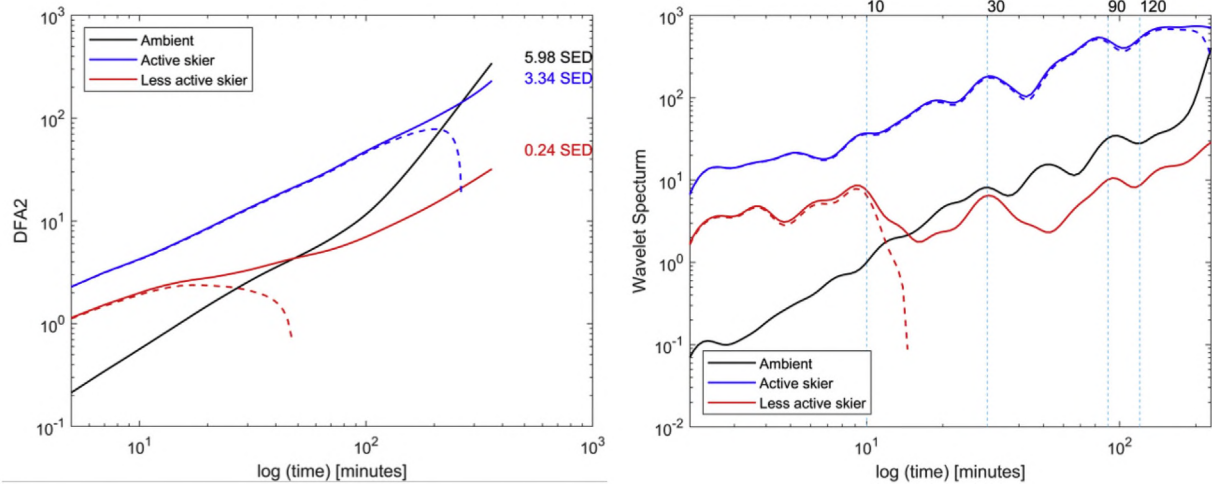


Fig. 4. DFA2 results, with values of total exposure in SED (left) and Morlet WT results (right) for an active skier (with dosimeter positioned on arm; blue lines) and less active skier (dosimeter positioned on head; red lines). Dashed lines represent the superposition of the respective result. Vertical dotted lines mark positions of cycles in pUVR data. (For interpretation of the references to colour in this figure legend, the reader is referred to the Web version of this article.)

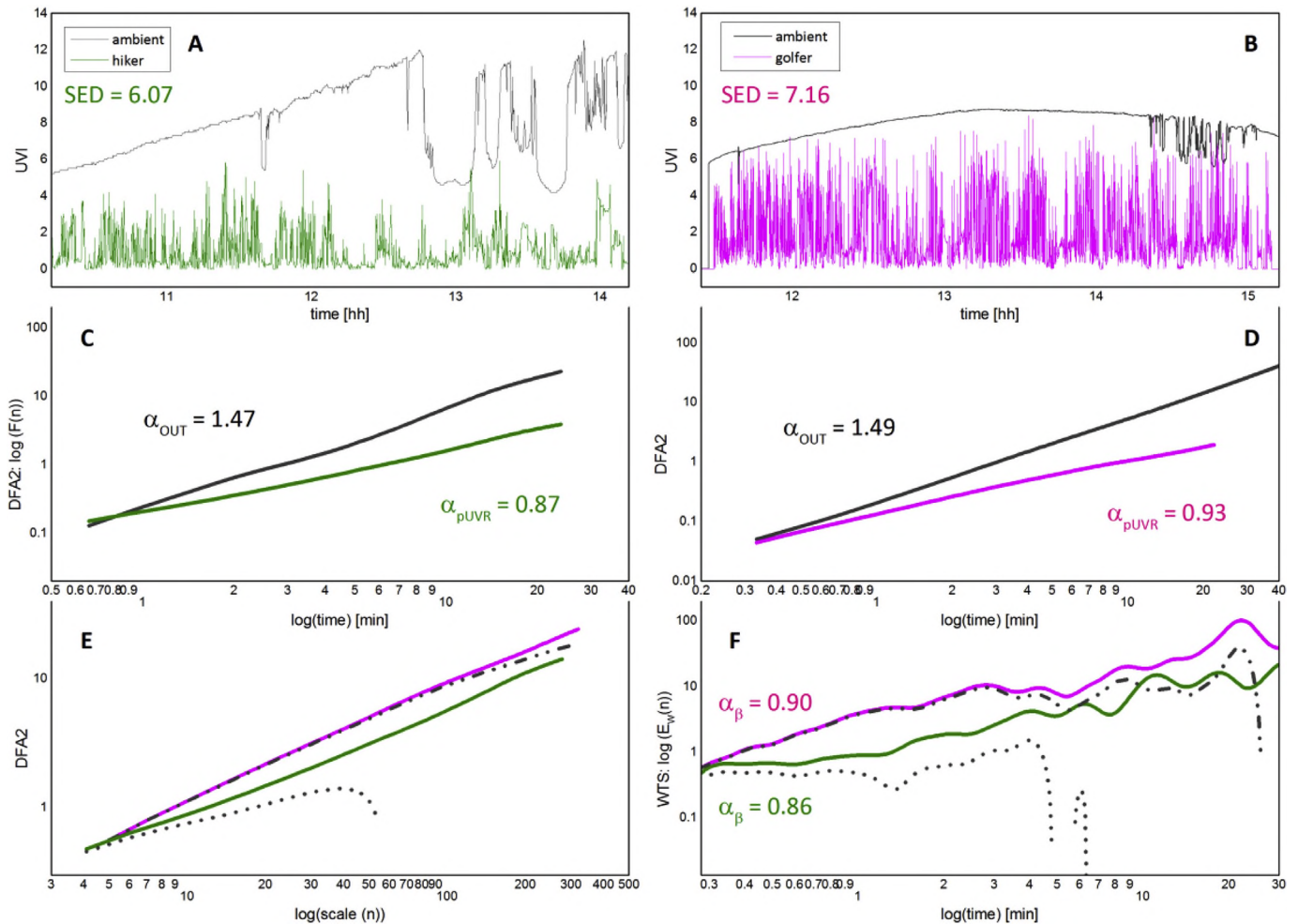
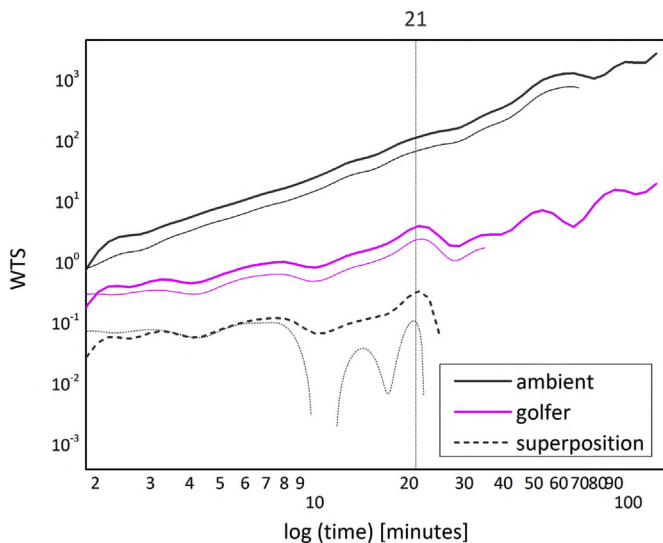


Fig. 5. (A) and (B) Data: original hiker and golfer pUVR measurements, together with the corresponding records of ambient UVR. Both sets of records are taken from wrist positions. Values of the total exposure for presented recording periods (in SED) are given. (C) and (D) DFA2 results: comparison of personal and ambient DFA2, for hiker and golfer data. Values of DFA2 exponents  $\alpha$  are given. (E) and (F): DFA-WTS results: comparison of DFA2 (E) and WTS (F) results for hiker and golfer data, together with functions derived from the superposition rule. DFA2 results in (E) are given as  $\log(F(N))$  vs  $\log(n)$ , to enable comparison of results; conversion of scale  $n$  into time  $t$  would, due to different rate of sampling in two experiments, translate DFA2 functions horizontally. Morlet wavelets were used for calculation in (F). Values of WTS exponents  $\beta$  in a form  $\alpha_\beta = (1 + \beta)/2$  are given.



**Fig. 6.** WTS functions for the golfer's pUVR, ambient, and 'personal' (from superposition) data, for the original 2-s recordings (thin lines) and averaged 1-min series (thick lines). Records are taken from golfer's hat.

Torrence and G. Compo and is available at URL: <http://atoc.colorado.edu/research/wavelets/>. We thank anonymous reviewers for stimulating comments.

## References

Allen, M., McKenzie, R., 2005. Enhanced UV exposure on a ski-field compared with exposures at sea level. *Photochem. Photobiol. Sci.* 4 (5), 429–437. <https://doi.org/10.1039/b418942f>.

Astafeva, N.M., 1996. Wavelet analysis: basic theory and some applications. *Phys. Uspekhi* 39 (11), 1085–1108. <https://doi.org/10.1070/PU1996v039n11ABEH000177>.

Baggerly, C.A., et al., 2015. Sunlight and vitamin D: necessary for public health. *J. Am. Coll. Nutr.* <https://doi.org/10.1080/07315724.2015.1039866>.

Bashan, A., et al., 2008. Comparison of detrending methods for fluctuation analysis. *Phys. A Stat. Mech. Appl.* 387 (21), 5080–5090. <https://doi.org/10.1016/j.physa.2008.04.023>.

Blesić, S., et al., 2018. Heterogeneity of scaling of the observed global temperature data. *J. Clim.* <https://doi.org/10.1175/JCLI-D-17-0823.1>.

Blesić, S.M., et al., 2016. Novel approach to analysing large data sets of personal sun exposure measurements. *J. Expo. Sci. Environ. Epidemiol.* 26 (6). <https://doi.org/10.1038/jes.2016.43>.

Bračić, M., Stefanovska, A., 1998. Wavelet-based analysis of human blood-flow dynamics. *Bull. Math. Biol.* 60 (5), 919–935. <https://doi.org/10.1006/bulm.1998.0047>.

Buldyrev, S.V., et al., 1995. Long-range correlation properties of coding and noncoding DNA sequences: GenBank analysis. *Physical Review E* 51 (5), 5084–5091. <https://doi.org/10.1103/PhysRevE.51.5084>.

Bunde, A., Bogachev, M.I., Lennartz, S., 2013. Precipitation and river flow: long-term memory and predictability of extreme events. In: *Extreme Events and Natural Hazards: the Complexity Perspective*, pp. 139–152. <https://doi.org/10.1029/2011GM001112>.

Chen, Z., et al., 2002. Effect of nonstationarities on detrended fluctuation analysis. *Phys. Rev. E Stat. Phys. Plasmas Fluids Relat. Interdiscip. Top.* 65 (4), 15. <https://doi.org/10.1103/PhysRevE.65.041107>.

Chen, Z., et al., 2005. Effect of nonlinear filters on detrended fluctuation analysis. *Phys. Rev. E - Stat. Nonlinear Soft Matter Phys.* 71 (1). <https://doi.org/10.1103/PhysRevE.71.011104>.

Cust, A.E., et al., 2018. Validation of questionnaire and diary measures of time outdoors against an objective measure of personal ultraviolet radiation exposure. *Photochem. Photobiol.* <https://doi.org/10.1111/php.12893>.

Fernández-Morano, T., et al., 2017. Sun exposure habits and sun protection practices of skaters. *J. Cancer Educ.* <https://doi.org/10.1007/s13187-016-1036-z>.

Gallagher, R.P., Lee, T.K., 2006. Adverse effects of ultraviolet radiation: a brief review. *Prog. Biophys. Mol. Biol.* <https://doi.org/10.1016/j.pbiomolbio.2006.02.011>.

Grossmann, A., Morlet, J., 1984. Decomposition of hardy functions into square integrable wavelets of constant shape. *SIAM J. Math. Anal.* 15 (4), 723–736. <https://doi.org/10.1137/0515056>.

Hacker, E., et al., 2018. Capturing ultraviolet radiation exposure and physical activity: feasibility study and comparison between self-reports, mobile apps, dosimeters, and accelerometers. *J. Med. Internet Res.* <https://doi.org/10.2196/resprot.9695>.

Hammond, V., Reeder, A.L., Gray, A., 2009. Patterns of real-time occupational ultraviolet

radiation exposure among a sample of outdoor workers in New Zealand. *Public Health.* <https://doi.org/10.1016/j.puhe.2008.12.007>.

Höll, M., Kantz, H., 2015. The relationship between the detrended fluctuation analysis and the autocorrelation function of a signal. *European Physical Journal B.* <https://doi.org/10.1140/epjb/e2015-60721-1>.

Höll, M., Kantz, H., Zhou, Y., 2016. Detrended fluctuation analysis and the difference between external drifts and intrinsic diffusionlike nonstationarity. *Physical Review E* 94 (4). <https://doi.org/10.1103/PhysRevE.94.042201>.

Hu, K., et al., 2001. Effect of trends on detrended fluctuation analysis. *Phys. Rev. E Stat. Phys. Plasmas Fluids Relat. Interdiscip. Top.* 64 (1), 19. <https://doi.org/10.1103/PhysRevE.64.011114>.

Islami, F., et al., 2017. 'Proportion and number of cancer cases and deaths attributable to potentially modifiable risk factors in the United States', CA. *A Cancer Journal for Clinicians.* <https://doi.org/10.3322/caac.21440>.

Jun, W.C., Oh, G., Kim, S., 2006. Understanding volatility correlation behavior with a magnitude cross-correlation function. *Phys. Rev. E - Stat. Nonlinear Soft Matter Phys.* <https://doi.org/10.1103/PhysRevE.73.066128>.

Kantelhardt, J.W., et al., 2001. Detecting long-range correlations with detrended fluctuation analysis. *Phys. A Stat. Mech. Appl.* 295 (3–4), 441–454. [https://doi.org/10.1016/S0378-4371\(01\)00144-3](https://doi.org/10.1016/S0378-4371(01)00144-3).

King, L., et al., 2015. Measuring sun exposure in epidemiological studies: matching the method to the research question. *J. Photochem. Photobiol. B Biol.* <https://doi.org/10.1016/j.jphotobiol.2015.10.024>.

Kiyono, K., 2015. Establishing a direct connection between detrended fluctuation analysis and Fourier analysis. *Phys. Rev. E - Stat. Nonlinear Soft Matter Phys.* <https://doi.org/10.1103/PhysRevE.92.042925>.

Koscielny-Bunde, E., et al., 2006. Long-term persistence and multifractality of river runoff records: detrended fluctuation studies. *J. Hydrol.* 322 (1–4), 120–137. <https://doi.org/10.1016/j.jhydrol.2005.03.004>.

Lucas, R.M., et al., 2008. Estimating the global disease burden due to ultraviolet radiation exposure. *Int. J. Epidemiol.* <https://doi.org/10.1093/ije/dyn017>.

Ludescher, J., Bunde, A., Schellnhuber, H.J., 2017. Statistical significance of seasonal warming/cooling trends. *Proc. Natl. Acad. Sci.* 114 (15), E2998–E3003. <https://doi.org/10.1073/pnas.1700838114>.

Mallat, S., Hwang, W.L., 1992. Singularity detection and processing with wavelets. *IEEE Trans. Inf. Theory* 38 (2), 617–643. <https://doi.org/10.1109/18.119727>.

Mandelbrot, B.B., Wallis, J.R., 1969. 'Some long-run properties of geophysical records'. *Water Resour. Res.* 5 (2), 321–340. <https://doi.org/10.1029/WR005i002p00321>.

Morlet, J., et al., 1982. Wave propagation and sampling theory; Part II, Sampling theory and complex waves. *Geophysics* 47 (2), 222–236. <https://doi.org/10.1190/1.1441329>.

O'Riordan, D.L., et al., 2008. A pilot study of the validity of self-reported ultraviolet radiation exposure and sun protection practices among lifeguards, parents and children. *Photochem. Photobiol.* <https://doi.org/10.1111/j.1751-1097.2007.00262.x>.

Peng, C.K., et al., 1993. Finite-size effects on long-range correlations: implications for analyzing DNA sequences. *Physical Review E* 47 (5), 3730–3733. <https://doi.org/10.1103/PhysRevE.47.3730>.

Peng, C.K., et al., 1994. Mosaic organization of DNA nucleotides. *Physical Review E* 49 (2), 1685–1689. <https://doi.org/10.1103/PhysRevE.49.1685>.

Perrier, V., Philipovitch, T., Basdevant, C., 1995. Wavelet spectra compared to Fourier spectra. *J. Math. Phys.* <https://doi.org/10.1063/1.531340>.

Seckmeyer, G., et al., 2012. A critical assessment of two types of personal UV dosimeters. *Photochem. Photobiol.* 88 (1), 215–222. <https://doi.org/10.1111/j.1751-1097.2011.01018.x>.

Da Silva Filho, P.C., Da Silva, F.R., Corso, G., 2016. Autocorrelation in ultraviolet radiation measured at ground level using detrended fluctuation analysis. *Phys. A Stat. Mech. Appl.* <https://doi.org/10.1016/j.physa.2016.01.039>.

Stanley, H.E., 2000. Exotic statistical physics: applications to biology, medicine, and economics. *Phys. A Stat. Mech. Appl.* 285 (1), 1–17. [https://doi.org/10.1016/S0378-4371\(00\)00341-1](https://doi.org/10.1016/S0378-4371(00)00341-1).

Stanley, H.E., 2005. Correlated randomness: some examples of exotic statistical physics. In: *Pramana, J. Phys.* pp. 645–660. <https://doi.org/10.1007/BF02704574>.

Stratimirović, D., et al., 2001. Wavelet analysis of discharge dynamics of fusimotor neurons. *Phys. A Stat. Mech. Appl.* 291 (1–4), 13–23. [https://doi.org/10.1016/S0378-4371\(00\)00495-7](https://doi.org/10.1016/S0378-4371(00)00495-7).

Stratimirović, D., et al., 2018. Analysis of cyclical behavior in time series of stock market returns. *Commun. Nonlinear Sci. Numer. Simul.* 54, 21–33. <https://doi.org/10.1016/j.cnsns.2017.05.009>.

Torrence, C., Compo, G.P., 1998. A practical guide to wavelet analysis. *Bull. Am. Meteorol. Soc.* 79 (1), 61–78. [https://doi.org/10.1175/1520-0477\(1998\)079<0061:APGTWA>2.0.CO;2](https://doi.org/10.1175/1520-0477(1998)079<0061:APGTWA>2.0.CO;2).

Wittlich, M., et al., 2016. An approximation of occupational lifetime UVR exposure: algorithm for retrospective assessment and current measurements. *J. Eur. Acad. Dermatol. Venereol.* <https://doi.org/10.1111/jdv.13607>.

Wright, C.Y., et al., 2007. Solar UVR exposure, concurrent activities and sun-protective practices among primary schoolchildren. *Photochem. Photobiol.* 83 (3), 749–758. <https://doi.org/10.1562/2006-08-22-RA-1010>.

Xiang, F., et al., 2015. Weekend personal ultraviolet radiation exposure in four cities in Australia: influence of temperature, humidity and ambient ultraviolet radiation. *J. Photochem. Photobiol. B Biol.* <https://doi.org/10.1016/j.jphotobiol.2014.12.029>.

Xu, L., et al., 2005. Quantifying signals with power-law correlations: a comparative study of detrended fluctuation analysis and detrended moving average techniques. *Phys. Rev. E - Stat. Nonlinear Soft Matter Phys.* 71 (5). <https://doi.org/10.1103/PhysRevE.71.051101>.